Citation: Cell Death and Disease (2012) 3, e330; doi:10.1038/cddis.2012.61

www.nature.com/cddis

Apoptosis, autophagy and ER stress in mevalonate cascade inhibition-induced cell death of human atrial fibroblasts

S Ghavami[1,2], B Yeganeh[1,2], GL Stelmack[1,2], HH Kashani[1,2], P Sharma[1,2], R Cunnington[3], S Rattan[3], K Bathe[3], T Klonisch[4], IMC Dixon[3,6], DH Freed[3,6] and AJ Halayko*[,1,2,5,6]

3-hydroxy-3-methyl-glutaryl-CoA reductase inhibitors (statins) are cholesterol-lowering drugs that exert other cellular effects and underlie their beneficial health effects, including those associated with myocardial remodeling. We recently demonstrated that statins induces apoptosis and autophagy in human lung mesenchymal cells. Here, we extend our knowledge showing that statins simultaneously induces activation of the apoptosis, autophagy and the unfolded protein response (UPR) in primary human atrial fibroblasts (hATF). Thus we tested the degree to which coordination exists between signaling from mitochondria, endoplasmic reticulum and lysosomes during response to simvastatin exposure. Pharmacologic blockade of the activation of ER-dependent cysteine-dependent aspartate-directed protease (caspase)-4 and lysosomal cathepsin-B and -L significantly decreased simvastatin-induced cell death. Simvastatin altered total abundance and the mitochondrial fraction of proapoptotic and antiapoptotic proteins, while c-Jun N-terminal kinase/stress-activated protein kinase mediated effects on B-cell lymphoma 2 expression. Chemical inhibition of autophagy flux with bafilomycin-A1 augmented simvastatin-induced caspase activation, UPR and cell death. In mouse embryonic fibroblasts that are deficient in autophagy protein 5 and refractory to autophagy induction, caspase-7 and UPR were hyper-induced upon treatment with simvastatin. These data demonstrate that mevalonate cascade inhibition-induced death of hATF manifests from a complex mechanism involving co-regulation of apoptosis, autophagy and UPR. Furthermore, autophagy has a crucial role in determining the extent of ER stress, UPR and permissiveness of hATF to cell death induced by statins.

Cell Death and Disease (2012) **3,** e330; doi:10.1038/cddis.2012.61; published online 21 June 2012
Subject Category: Internal Medicine

Structural remodeling of the heart tissue, including fibrosis, cardiomyocyte death, hypertrophy of surviving myocytes and proliferation of cardiac fibroblasts, is a feature of cardiac disease, heart failure and atrial fibrillation.[1] Cardiac fibroblasts account for about two-thirds of the cells in the normal heart, and maintain cardiac integrity during physiologic proliferation and extracellular matrix turnover, and during cardiac remodeling. They exhibit phenotype plasticity and have the capacity for phenoconversion from a quiescent state (healthy heart) to a proliferative myofibroblast phenotype, acquiring specialized contractile features in the diseased heart.[2,3] This characteristic is the basis of tissue remodeling during normal and pathologic wound healing associated with myocardial infarction, heart failure and atrial fibrillation.

Although statins are widely used in cardiovascular disease prevention to lower cholesterol, they have other effects unrelated to lipid reduction that are essential for their positive impact on human health.[4,5] A number of studies show that statin use is protective against maladaptive tissue remodeling and of benefit against heart failure.[6,7] Statins inhibit 3-hydroxy-3-methyl-glutaryl-CoA (HMG-CoA) reductase, the proximal rate-determining enzyme in the multi-step mevalonate cascade for cholesterol synthesis. Mevalonate is used for cholesterol biosynthesis via squalene, but is also a precursor for isoprenoids (farnesyl pyrophosphate (FPP) and geranylgeranyl pyrophosphate (GGPP)). FPP and GGPP are substrates for farnesylation of H-Ras and geranylgeranylation of RhoA, post-translational modifications

[1]Department of Physiology, University of Manitoba, Winnipeg, Manitoba, Canada; [2]Manitoba Institute of Child Health, University of Manitoba, Winnipeg, Manitoba, Canada; [3]Institute of Cardiovascular Sciences, University of Manitoba, Winnipeg, Manitoba, Canada; [4]Department of Human Anatomy and Cell Science, University of Manitoba, Winnipeg, Manitoba, Canada and [5]Department of Internal Medicine, University of Manitoba, Winnipeg, Manitoba, Canada
*Corresponding author: AJ Halayko, Departments of Physiology and Internal Medicine, University of Manitoba, 745 Bannatyne Avenue, 810 Sherbrook Street, Winnipeg, Manitoba R3E 0W3, Canada. Tel: +1 204 787 2062; Fax: +1 204 789 3915; E-mail: ahalayk@cc.umanitoba.ca
[6]These authors have equal senior authorship.
Keywords: simvastatin; unfolded protein response; heart; lysosome; cardiac remodeling
Abbreviations: ATF6, activating transcription factor 6; ATG5, autophagy protein 5; BAD, Bcl-2-associated death promoter protein; BAK, BCL-2-antagonist/killer; BAX, Bcl-2-associated X protein; Bcl-2, B-cell lymphoma 2; BID, BH3-interacting domain death agonist; BNIP3, Bcl-2 19 kDa-interacting protein 3; Caspases, cysteine-dependent aspartate-directed proteases; CHOP, C/EBP homologous protein; ER, endoplasmic reticulum; FPP, farnesyl pyrophosphate; GGPP, geranylgeranyl pyrophosphate; hATF, human atrial fibroblast; HMG-CoA reductase, 3-hydroxy-3-methyl-glutaryl-CoA reductase; IAP, inhibitor of apoptosis protein; IREα1, inositol-requiring enzyme alpha 1; JNK/SAPK, c-Jun N-terminal kinase/stress-activated protein kinase; LC3, microtubule-associated protein light chain 3; LSC, laser scanning cytometer; PERK, protein kinase-like endoplasmic reticulum kinase; PUMA, p53 upregulated modulator of apoptosis; TEM, transmission electron microscopy; UPR, unfolded protein response; XBP1, X box-binding protein 1
Received 06.1.12; revised 11.4.12; accepted 23.4.12; Edited by M Federici

that enable membrane localization and activation of small GTPases.[8,9]

Mevalonate depletion can induce apoptosis, autophagy and endoplasmic reticulum (ER) stress in cancerous[10] and noncancerous cells.[11,12] In lung mesenchymal cells mevalonate cascade inhibition activates apoptosis by a process involving p53, disruption of mitochondrial fission and release of proteins that interfere with inhibitor of apoptosis proteins (IAP).[13] Simvastatin and a geranylgeranyl transferase I inhibitor induce autophagy and apoptosis, but the response is balanced by the p53 regulatory network.[12,14]

Despite the role of fibroblasts in cardiac pathologies, direct effects of mevalonate cascade inhibition on human atrial cardiac fibroblast function have not been well studied. Therefore, here we investigated cell death mechanisms linked to mevalonate cascade inhibition in human atrial fibroblasts (hATF), focusing on apoptosis, autophagy and ER stress. This study dissects the concomitant interplay between these cellular events and their impact on human atrial fibroblast fate in response to its clinically relevant stimulus, simvastatin. Our results could influence direction for therapy related to cardiac fibrosis.

Results

Mevalonate cascade inhibition induces cholesterol-independent cell death. We first identified concentration- (0–20 μM) and time-dependent (0–96 h) effects of simvastatin exposure on primary hATF cells. 3-(4,5-dimethyl-2-thiazolyl)-2,5-diphenyl-2H-tetrazolium bromide (MTT) assay (Figure 1a) revealed that all concentrations of simvastatin up to 20 μM significantly induced cell death in primary hATF cells after 48 and 96 h ($P<0.001$). Further experiments showed that though exogenous mevalonate (2.5 and 5 mM) significantly blunted both simvastatin-induced cell death ($P<0.001$) (Figure 1b) and morphological changes in hATF cells (Figure 1c), co-treatment with cholesterol was not sufficient to prevent simvastatin-induced cell death ($P>0.5$) (Figure 1d). Thus, the simvastatin-triggered toxicity relied upon mevalonate depletion, but not on suppression of cholesterol synthesis *per se*. As several reports indicate that inhibiting the mevalonate cascade is associated with reduced membrane anchoring of small GTPase signaling proteins to contribute to statin-provoked cell death,[13,15] we next assessed the impact of simvastatin treatment on membrane localization of RhoA, RhoC and Rac1/2/3. Simvastatin effectively reduced the abundance of these proteins in plasma membrane fraction while increasing cytosolic content (Figure 1e).

Mevalonate cascade inhibition activates the intrinsic apoptotic pathway. SC scattergrams were collected after treating hATF with simvastatin (10 μM, 48 and 96 h) (Figure 2a). The induction of chromatic condensation without loss of total nuclear DNA, features of apoptosis, was evident from marked increase in the maximum pixel fluorescence of cells labeled with H33342 DNA dye. This was confirmed by examining 'gallery photos' of individual nuclear events from relevant scattergram quadrants (Figure 2b). Quantitative analysis of laser scanning cytometer (LSC) scattergrams demonstrated that simvastatin treatment (10 μM, 48 and 96 h) significantly activated apoptosis in primary hATF (Figure 2c).

To investigate the effects of mevalonate cascade inhibition on both extrinsic and intrinsic apoptosis pathways, we measured cysteine-dependent aspartate-directed proteases (caspase) cleavage in hATF following simvastatin treatment for up to 120 h (Figure 2d). Caspase-9 cleavage, a marker of activation of the intrinsic apoptosis pathway was evident within 24 h and increased steadily thereafter. Cleavage of caspase-3, -6 and -7 was also induced by statin exposure after 48 h, indicating that apoptosis was ongoing after the initial caspase-9 induction. We also examined activation of the extrinsic apoptosis pathway by assessing Bid and found no evidence for its cleavage to t-Bid (Figure 2d) or for cleavage of caspase-8 (data not shown). Collectively these data show that intrinsic apoptosis activation occurs selectively upon mevalonate cascade inhibition.

Mevalonate cascade inhibition increases autophagy and activates lysosomes. Statins can induce autophagy in different cell models.[12,16] Here, we show that simvastatin induces autophagy in hATF. First, analysis of ultrastructure after statin exposure showed an increase in autophagosome number (Figure 3a). Second, multiple protein markers of autophagy were induced by simvastatin treatment: these included microtubule-associated protein light chain 3β (LC3β) lipidation,[17] ubiquitination-dependent Atg5-12 formation[18] and beclin-1 expression[19] (Figure 3b). Third, we investigated lysosomal activation (increase in lysotracker red staining) and formation of LC3 punctae and found that simvastatin exposure markedly induced these responses (Figures 3c and d). We also found that simvastatin induced pronounced cathepsin-B and -L cleavage (Figure 3e). Furthermore, we observed that specific inhibitors of cathepsin-B (CA-074-OME) and cathepsin-B/L (z-FF-FMK) significantly decreased simvastatin-induced cell death in hATF ($P<0.001$) (Figures 3f and g). This confirms the involvement of cathepsin-B and -L in simvastatin-induced cell death.

Mevalonate cascade inhibition promotes the unfolded protein response (UPR). ER stress develops in response to harsh environmental cues and the UPR is induced to facilitate adaptation to the changing environment and re-establish homeostasis and ER function. We measured the impact of simvastatin exposure on expression and activation of ER stress sensors and markers, including BIP (GRP78), inositol-requiring enzyme alpha 1 (IREα1), activating transcription factor 6 (ATF6) and protein kinase PERK (protein kinase-like endoplasmic reticulum kinase), which mediate the activation of the UPR in mammalians cells.[20] As shown in Figure 4a, mevalonate cascade inhibition leads to increased expression of BIP (GRP78) and IREα1, cleavage of ATF6 and phosphorylation of PERK. The activation of the UPR ultimately leads to the attenuation of protein translation (eIF2α phosphorylation), X box-binding protein 1 (XBP1) splicing and increased expression of C/EBP homologous protein (CHOP), a protein that links chronic ER stress to apoptosis.[21] Figure 4a further demonstrates that each of these UPR-triggered responses is induced in hATF upon simvastatin exposure. Furthermore, nuclear accumulation of

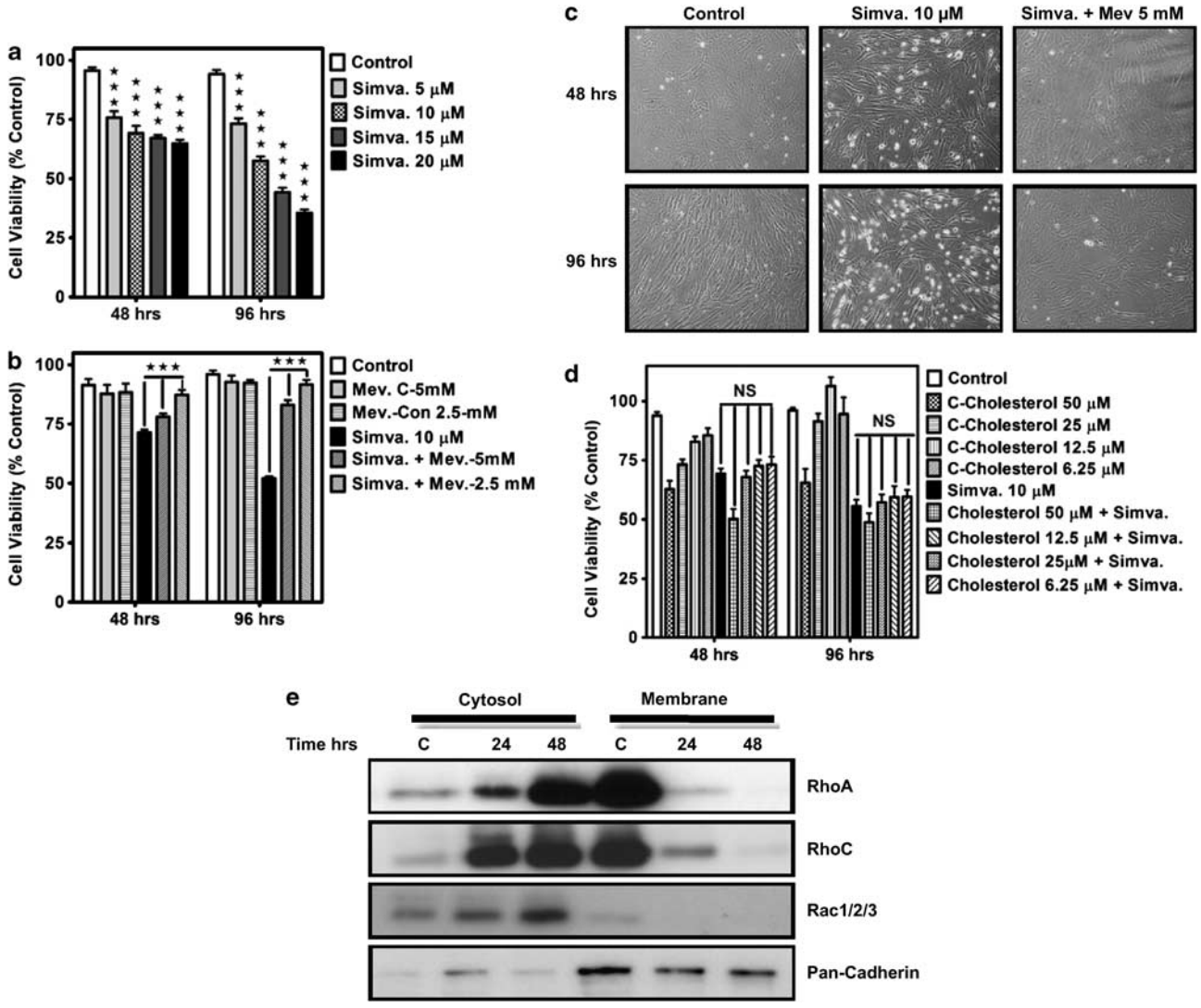

Figure 1 Mevalonate cascade inhibition induces cell death in primary myocardial atrial fibroblast. (**a**) Cells were treated with simvastatin (5, 10, 15 or 20 μM) and cell viability was assessed 48 and 96 h thereafter by MTT assay. Control cells for each time point were treated with the solvent control (DMSO). Results are expressed as percentage of corresponding time point control and represent the mean ± S.D. of nine independent experiments in three different of patient myocardial atria fibroblast (***$P<0.001$). (**b** and **c**) Effects of supplementation with 2.5 and 5 mM mevalonate on cell viability (MTT Assay) (**b**) and cell morphology (**c**), to treatment with simvastatin (10 μM, 48 and 96 h) on simvastatin-induced cell death. Cells were pretreated with indicated concentration of mevalonate (4 h) and then co-treated with simvastatin (10 μM, 48 and 96 h). For each experiment control cells were treated with simvastatin and mevalonate solvent (DMSO and ethanol) alone. Results are expressed as mean ± S.D. of nine independent experiments using three different myocardial atrial fibroblast primary cells (***$P<0.001$). (**d**) Effects of supplementation with cholesterol (0–50 μM) on cell viability (MTT Assay), with simvastatin (10 μM, 48 and 96 h). Cells were pretreated with indicated concentration of cholesterol (4 h) and then co-treated with simvastatin (10 μM, 48 and 96 h). For each experiment control cells were treated with simvastatin and cholesterol solvent (DMSO and ethanol) alone (control) or with both. Results are expressed as mean ± S.D. of nine independent experiments using three different myocardial atrial fibroblast primary cells (NS, non significant). (**e**) Time course of simvastatin (10 μM) on the abundance of RhoA, RohC and Rac1/2/3 and in membrane and cytosolic fractions obtained from myocardial fibroblast (western blot). Presence of pan-Cadherin was used to normalize for loading of membrane fractions. Data are typical of two independent experiments using different primary cultures

the UPR-related transcription factors, ATF4, cleaved ATF6 and spliced XBP1 was evident (Figure 4b). In many cell types the UPR is also associated with activation of ER-associated, caspase-4 [22,23] and its expression and cleavage is increased during ER stress;[24] we confirmed that this was the case with mevalonate cascade inhibition in hATF (Figure 4c). To confirm that caspase activation was a component of ER-linked cell death we tested the impact of specific inhibitors of caspase-4 (Z-LEVD-FMK, 10 μM) on simvastatin-induced cell death with lowest possible effective concentration based on our experience and that of others[23,25] and found that they could partially prevent loss of cell viability ($P<0.001$) (Figure 4d) in concert with suppressive effects on caspase-3/7 activity (Figure 4e).

Exogenous mevalonate suppresses simvastatin-induced, autophagy, UPR and apoptosis. We questioned whether co-incubation of simvastatin-treated cells with mevalonate could prevent the apoptotic, autophagic and/or UPR responses. By immunoblotting we observed that

exogenous mevalonate inhibited markers of the autophagy response (LC3β-lipidation), UPR (eIF2α-phosphorylation, IREα1, ATF4 expression, ATF6 cleavage) and apoptosis (caspase-3 and -7 cleavage) (Figures 5a and b). These findings are consistent with data in Figure 1b that indicate exogenous mevalonate prevents simvastatin-induced loss of hATF viability.

Mevalonate cascade inhibition affects B-cell lymphoma 2 (Bcl-2) protein expression and decreases mitochondrial membrane potential. Bcl-2 family proteins regulate apoptosis via modulation of mitochondrial outer membrane integrity: Bcl-2 and Bcl-XL prevent the release of apoptogenic proteins from mitochondria, whereas Bax, Bak, Bad, PUMA and NOXA induce outer membrane permeabilization causing the release of proapoptotic factors.[26] We examined differential expression of Bcl-2 family proteins in simvastatin-treated hATF. Mevalonate cascade inhibition decreased abundance of antiapoptotic Bcl-2 and Mcl-1 while increasing proapoptotic Bax, NOXA, PUMA, BNIP3 (30 and 60 kDa) and BAD in whole-cell lysates (Figure 6a). Simvastatin caused Bax accumulation in cytosolic fractions, and in mitochondria-enriched fractions there was

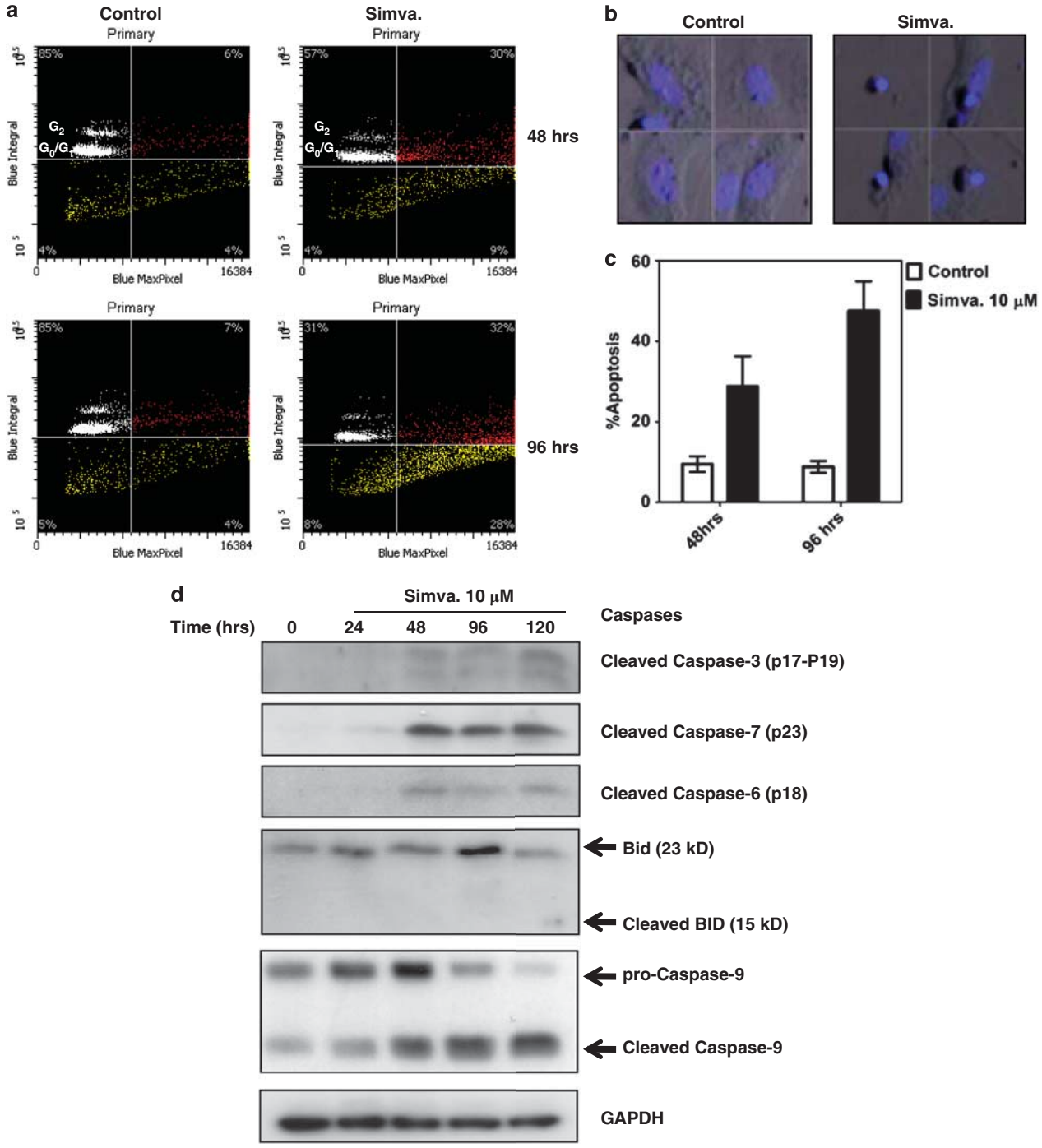

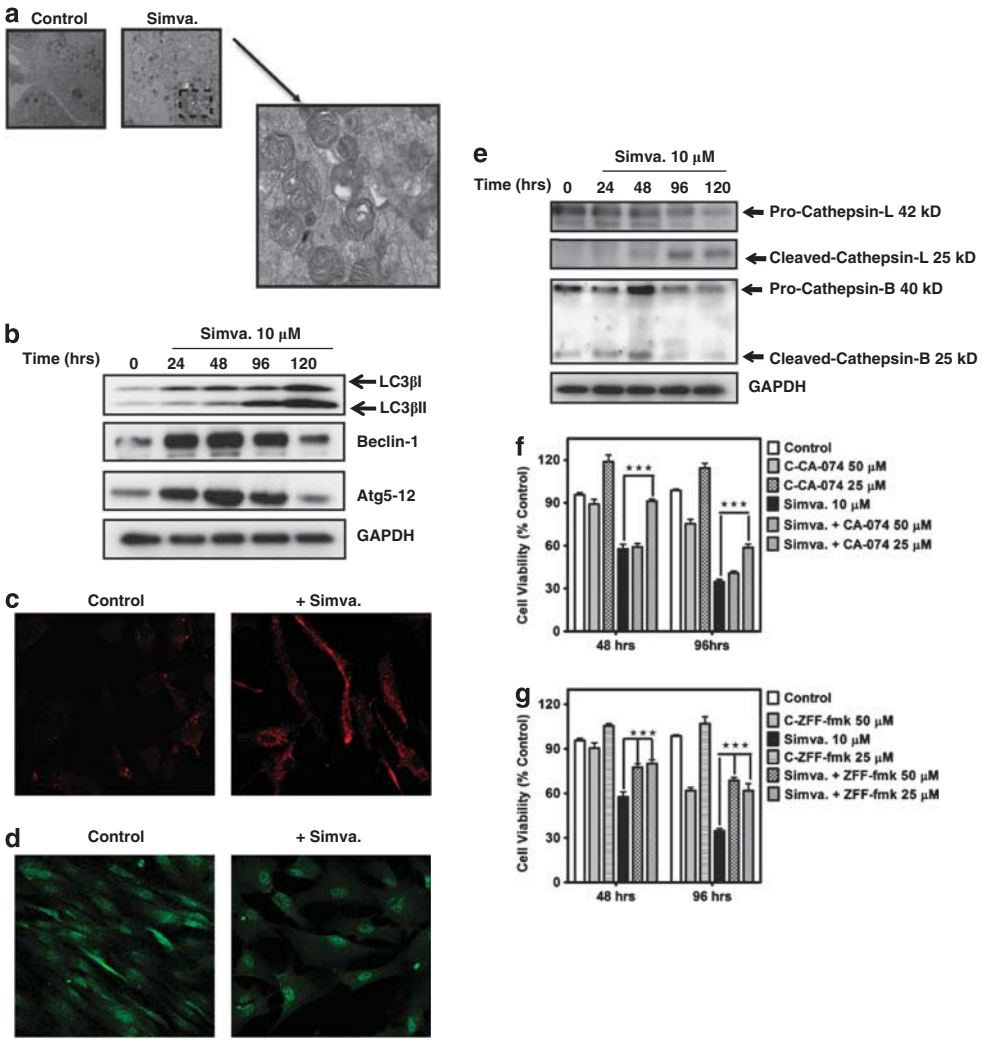

Figure 3 Mevalonate cascade stimulates autophagy in primary human myocardial atrial fibroblast. (**a**) Myocardial atrial fibroblast cells were either left untreated (top left) or they were treated with 10 μM simvastatin (top right, and lower panels) for 72 h. Cells were then imaged by TEM. Magnification: 3.4×10^3. Structures identified as autophagosomes can be seen as double-membrane vacuoles in magnified part of the figures. (**b**) Western blot analysis of cell lysates from myocardial atrial fibroblast. Cells were treated with 10 μM simvastatin for the indicated time periods, and then immunoblotted using the indicated specific antibodies. GAPDH was used as loading control. (**c**) Myocardial atrial fibroblast treated with simvastatin (+ Simva, 10 μM, 72 h) showed increased Lysotracker Red staining, a marker of lysosomal activation. (**d**) Myocardial atrial fibroblast cells treated with simvastatin showed an increase in LC3-β (green) punctuate indicating autophagosome formation. (**e**) Western blot analysis of cell lysates from myocardial atrial fibroblast cells. Cells were treated with 10 μM simvastatin for the indicated time points and then immunoblotted using the indicated specific antibodies. Simvastatin induced late cathepsin L and early cathepsin-B activation. (**f** and **g**) Myocardial atrial fibroblast were pretreated with specific cathepsin-B inhibitor (CA-074, 4 h, **f**) or cathepsin-B and -L inhibitor (ZFF-fmk, 4 h, **g**) and then co-treated with simvastatin (10 μM) for indicated time points. Cell viability was measured using MTT assay. Cathepsin inhibitors significantly inhibited simvastatin-induced cell death in myocardial atrial fibroblast (***$P < 0.001$)

Figure 2 Mevalonate cascade inhibition stimulates intrinsic caspase-dependent apoptosis in primary myocardial atrial fibroblast. (**a**) Examples of typical scattergrams obtained by LSC of myocardial fibroblast cells treated with vehicle control or 10 μM simvastatin for 48 and 96 h. *y* axis data represent total integrated fluorescence of individual events (nuclei) and *x* axis shows maximum pixel fluorescence intensity within each event contour. Horizontal axis in each scattergram represents the threshold determined for reliable event identification, and the vertical line represents the outer boundary for normal cell pixel intensity (determined from control data). The position of cells with diploid or tetraploid nuclear DNA, representing G_0/G_1 or G_2 cell cycle phase, is indicated in each scattergram. Percentages shown in upper quadrants indicate the mean % of cells determined from three separate experiments. Event frequency from color-coded ROI's from scattergrams are used to populate the histogram in panel 2c (below). Color-coding: White region represents healthy cells with integrated (2 N or 4 N) nuclear fluorescence in the G0/G1 and G2 phase of the cell cycle; Red region represent cells in which nuclear condenstation has occurred, and likely represent cells in early apoptosis (shifted right on *X*-axis for maximum pixel nuclear flurescence); and, Yellow region represents cells with reduced integrated nuclear fluorescence (DNA cleavage), and includes cells that exhibit more advanced apoptosis (increasing DNA cleavage and loss of DNS condensation), that correspond to a subG0/G1 population. (**b**) Galleries of images for individual cells representing events for 'healthy' hATF (from the white color-coded region in **a**) and simvastatin-treated (10 μM, 96 h) 'early apoptotic' cells G_0/G_1 cells (from the red color-coded region in **a**). (**c**) Histogram summarizing % apoptosis of cells extracted from LSC scattergrams of control and simvastatin-treated hATF (10 μM, 96 h). Apoptotic cell counts included the sum of hATFs from both the red and yellow colored regions of scattergrams (e.g. **a**). Results represent three different independent experiments in two different sets of primary atrial fibroblast. (**d**) Immunoblot BID, cleaved caspase-3, -6, -9 and -7 in total cell lysates of primary myocardial fibroblast. Cells were treated with simvastatin (10 μM) for up to 120 h. Arrows indicate positions and approximate molecular weight of predicted and visible protein signals. For all lanes GAPDH was used as protein loading control. Blots are typical of three experiments completed using different patient cultures of atrial fibroblast

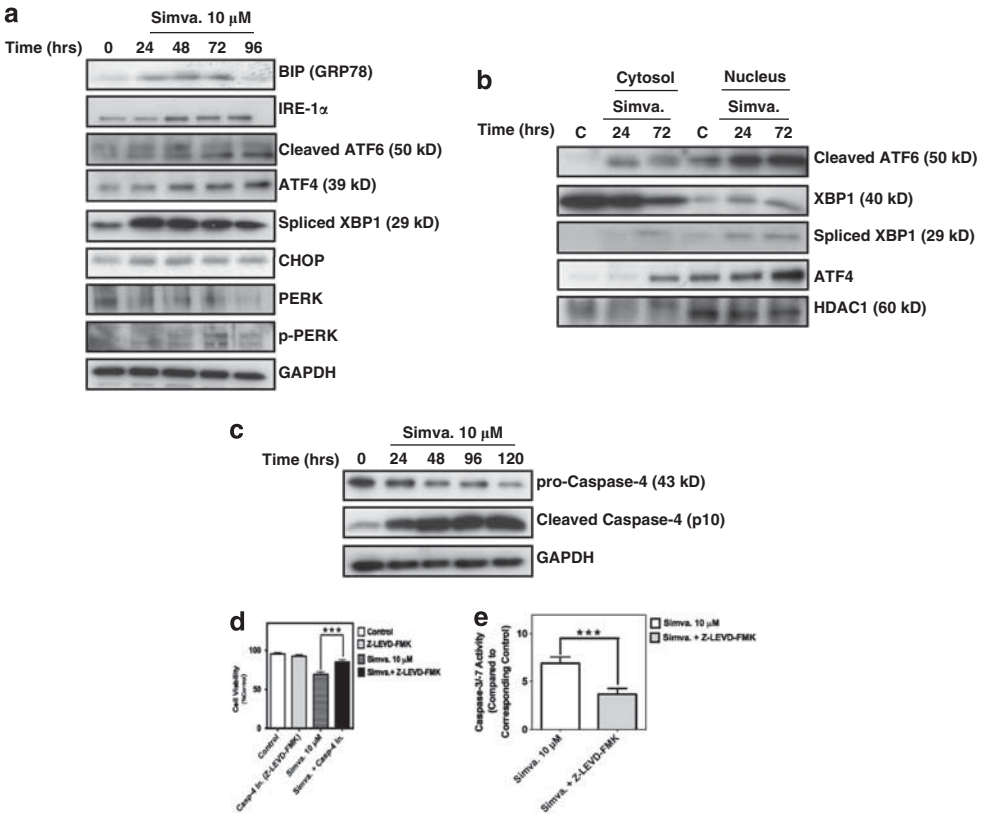

Figure 4 Mevalonate cascade inhibition induces endoplasmic reticulum stress and activates UPR in primary human myocardial atrial fibroblast. (**a**) Western blot analysis of cell lysates from myocardial atrial fibroblasts. Cells were treated with 10 μM simvastatin before sample preparation at the indicated times. Immunoblotting was performed using the indicated specific antibodies. Simvastatin increased the expression of IREα1, CHOP and ATF4 and enhanced ATF6 cleavage, XBP1 splicing, eif2α and PERK phosphorylation. Equal protein loading was confirmed by detecting GAPDH protein. (**b**) Simvastatin increased nuclear accumulation of endoplasmic reticulum-related proteins. Cells were treated with simvastatin (10 μM) for indicated time point and cytosolic and nuclear fractions were prepared. Simvastatin increased ATF4, cleaved ATF6 and spliced XBP1 nuclear content. HDAC1 was used to assess fraction purity and as an equal loading control. (**c**) Simvastatin activated endoplasmic reticulum-related caspase. Cells were treated with simvastatin then cell lysates were probed for caspase-4 cleavage by immunoblot. Simvastatin induced caspase-4 activation. Equivalent loading was confirmed using GPADH. (**d** and **e**) Myocardial atrial fibroblasts were pretreated with caspase-4 inhibitor (Z-LEVD-FMK, 10 μM) for 4 h and then co-treated with simvastatin (10 μM, 96 h). Cell viability was measured using MTT assay. Caspase-4 inhibitor significantly decreased simvastatin-induced cell death and caspase-3/-7 activation (**f**) (***$P<0.001$)

accumulation of proapoptotic Bax, PUMA, NOXA and BNIP3 with concomitant loss of antiapoptotic Bcl-2, Mcl-1 and Bcl-XL (Figure 6b). In concert with accumulation of proapoptotic proteins in mitochondria, mitochondrial membrane potential ($\Delta\psi$) was also decreased (Figure 6c).

c-Jun N-terminal kinase/stress-activated protein kinase (JNK/SAPK) signaling appears to promote decreased Bcl-2 expression and subsequent apoptosis induction in some cell types, and chronic UPR reportedly triggers JNK/SAPK activation.[20,27] Thus, we examined whether simvastatin-induced loss of Bcl-2 is associated with and dependent on JNK/SAPK activation. Indeed, mevalonate cascade inhibition caused JNK/SAPK phosphorylation (Figure 6d), and the specific JNK/SAPK inhibitor, SP600125 (150 nM, 72 h), concomitantly inhibited simvastatin-induced cell death ($P<0.01$) (Figure 6e) and loss of antiapoptotic Bcl-2 (Figure 6f). Taken together, these data indicate altered Bcl-2 family expression is linked to mevalonate cascade inhibition-induced cell death, and this is, in part, associated with JNK/SAPK activation that prevents loss of Bcl-2.

Autophagy negatively regulates mevalonate depletion-induced apoptosis and UPR. We used two approaches to assess whether autophagy inhibition may regulate mevalonate cascade-dependent apoptosis and UPR: (1) chemical inhibition of autophagy flux by preventing autophagosome-lysosome fusion with bafilomycin-A1; and, (2) assessing responses in autophagy protein 5 (ATG5)-deficient mouse embryo fibroblasts (*ATG5* KO MEF). Bafilomycin-A1 augmented simvastatin-induced LC3β II accumulation, indicating that autophagy flux was prevented (Figure 7a). Notably, this was accompanied by an increase in caspase-7 and -9 activation and increased in BIP and IREα1, indicating apoptosis and UPR responses were augmented by autophagy inhibition. Consistent with these data, bafilomycin-A1 also significantly ($P<0.001$) increased mevalonate cascade inhibition-induced cell death in hATF (Figure 7b).

ATG5 conjugates with ATG12 and associates with isolated membranes to form autophagosomes.[28] Though the extent to which *ATG5* KO MEF may undergo some form of adaption is not easily discerned, we did observe that mevalonate cascade

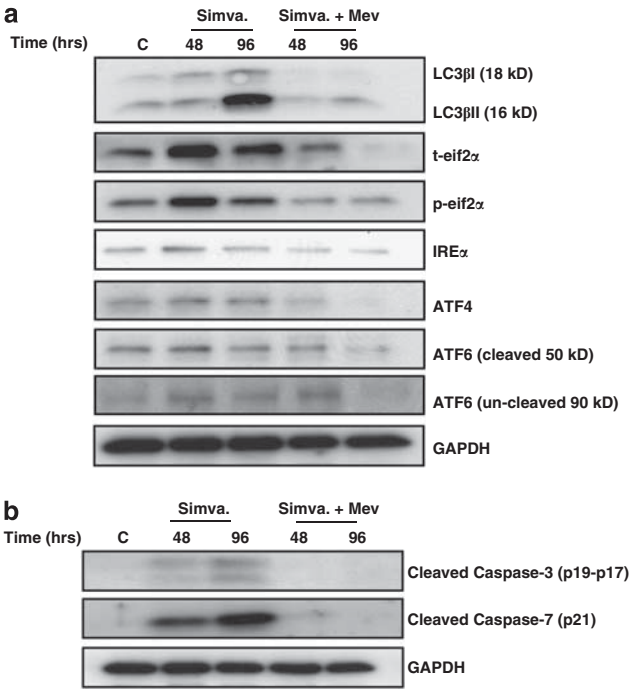

Figure 5 Mevalonate inhibits simvastatin-induced autophagy, endoplasmic reticulum stress and apoptosis. Myocardial atrial fibroblast were pretreated with mevalonate (2.5 mM, 4 h) and then co-treated with simvastatin (10 μM) for indicated time points. Immunoblots of cell lysates showed inhibition of (**a**) autophagy, endoplasmic reticulum stress and (**b**) apoptosis markers

inhibition resulted in a significantly greater degree of cell death compared with wild-type MEF ($P<0.001$) (Figure 7c). This was associated with greater caspase-7 activation and higher BIP (GRP78) expression (Figure 7d). This data further reveal that autophagy negatively regulates mevalonate cascade-induced apoptosis and UPR.

Discussion

Disruption of the mevalonate cascade reportedly affect apoptosis, autophagy and UPR/ER stress in cancerous and noncancerous cells, but the simultaneous interactions between the three responses are not described. The current study demonstrates and deciphers interplay between these cellular stress responses upon exposure to a clinically relevant mevalonate cascade inhibitor, simvastatin, and does so in primary cultured hATF. As such, in these cells we provide first time insight concerning apoptosis and ER stress pathways, and the modulating impact of autophagy, which ultimately was not sufficient to prevent cell death. Figure 8 summarizes the coordinated interactions we uncovered, and discuss hereafter. Our data are relevant as induction of apoptosis in myofibroblasts diminish their number in myocardium and may be modulated by autophagy, thus regulating the potential for extracellular matrix deposition in the diseased myocardium.

Our findings highlight a possible role for isoprenoid intermediates of the mevalonate cascade in cell function and survival. Simvastatin-induced cell death of hATF is not mediated by reduced cholesterol synthesis *per se*, rather is tied to limiting the availability of isoprenoid chains needed for membrane anchoring of Ras superfamily GTPases. This is consistent with other reports, including our own on human lung mesenchymal cells.[12,29] In the present study, we demonstrate that simvastatin limits the expression of the antiapoptotic protein, Bcl-2, an effect associated with JNK/SAPK activation (Figure 8). Moreover, mevalonate cascade inhibition induces apoptosis, UPR/ER stress and release of activated lysosomal cathepsins. These responses are restricted by a simultaneous induction of autophagy flux. These insights are important, given the long-term usage of statins in the general population, as we unveil cellular responses that could be associated with clinical effects of statins.

Consensus on the effect of statins on UPR and ER stress has not been reached, in part because of the broad range of intracellular effects caused by mevalonate cascade inhibition in different cell types. Statins can inhibit ER stress,[30] but reportedly can also activate UPR and ER stress,[11,31] whereas other studies report no effect on UPR and ER stress.[32] These inconsistencies suggest that mevalonate cascade-associated regulation of UPR and ER stress may be conditional on the cells studied and experimental conditions, for instance metabolic changes that can develop upon cell transformation. In hATF we found simvastatin increased spliced XBP1, a response that has not yet been clearly linked to specific functional responses in different cells.[33] Nonetheless, it may be an early cell survival response or could activate other signaling pathways during statin-induced ER stress. Further investigation is needed to elucidate how statin-induced XBP1 splicing affects cell response and fate.

The UPR is thought to be adaptive, re-establishing homeostasis and normalizing ER function in a changing environment. UPR activation triggers transcriptional responses that increase expression of genes encoding products that adjust ER protein folding capacity and ER-assisted protein degradation. Without homeostatic balance, the cell dies,[34] thus triggering the UPR that can result in cell adaptation, alarm or apoptosis.[20] Our results show that mevalonate cascade inhibition induces UPR: increased IREα1 and BiP/GRP78, cleavage of ATF6, phosphorylation of PERK, XBP1 splicing and nuclear accumulation of ATF4 and ATF6 (Figure 8). This is accompanied by the accumulation of CHOP (also known as growth-arrest and DNA damage inducible gene 153 (GADD153)), a protein initially linked with responses to DNA damage.[35] The gene promoter for CHOP contains regulatory elements for inducers of the UPR, including ATF4 and ATF6.[36] CHOP regulates transcription of genes encoding Bcl-2 family proteins[37] and can provoke caspase activation, thus triggering cell demise. In the context of our studies, statin exposure could trigger UPR and Bcl-2 protein-mediated apoptosis via pathways involving CHOP.

We show that other pathways also contribute to altered Bcl-2 expression in statin-treated hATF (Figure 8). Bcl-2 family proteins regulate cell death, carrying out their function by controlling mitochondrial permeability. We found that mevalonate cascade inhibition promoted accumulation and mitochondrial association of proapoptotic Bcl-2 proteins (Bax, Bad, PUMA, NOXA and BNIP3), whereas there was a decrease in cytosolic abundance of antiapoptotic Bcl-2

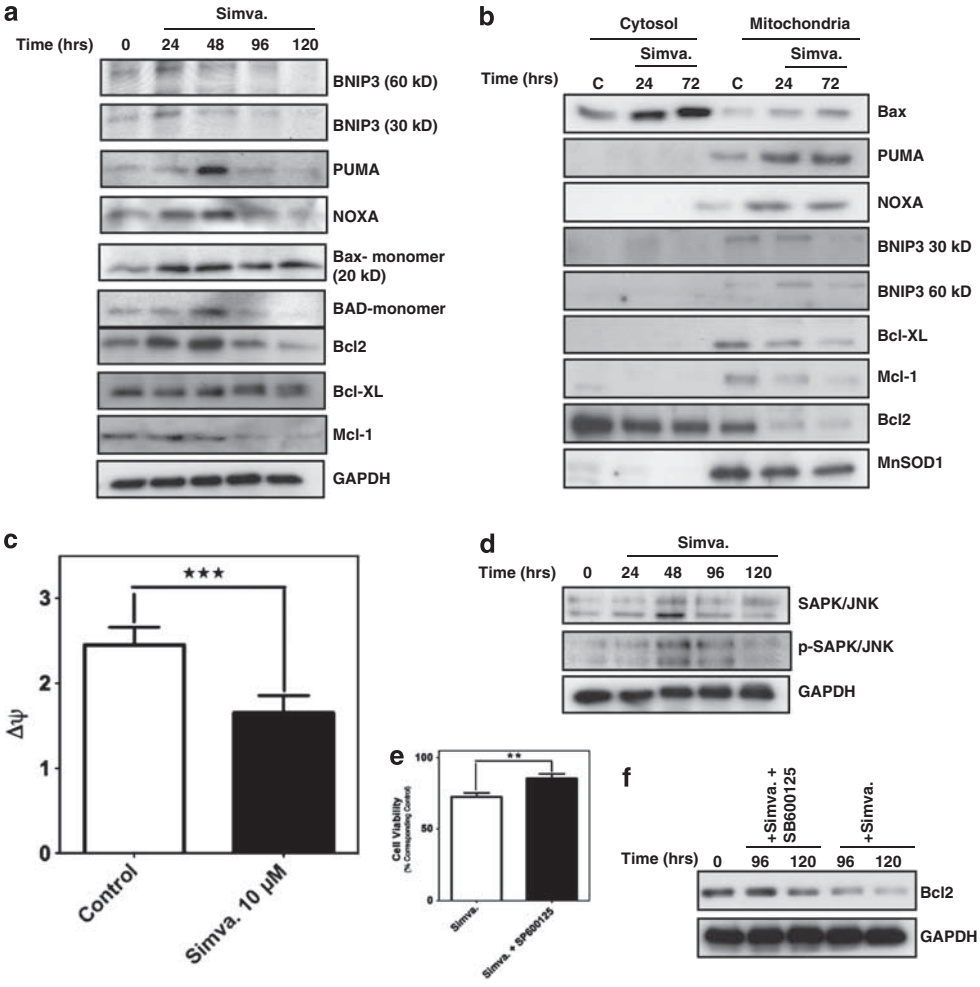

Figure 6 Mevalonate cascade inhibition changes the balance and localization of anti and proapoptotic Bcl-2 family member and affects mitochondrial membrane potential in myocardial atrial fibroblast. (**a** and **b**) Myocardial atrial fibroblasts were treated with simvastatin (10 μM) for indicated times and pro and antiapoptotic Bcl-2 family member expression and localization (cytosolic/mitochondria-enriched fraction) were investigated using immunoblotting. Mevalonate cascade inhibition increased proapoptotic Bcl-2 family member expression and their mitochondrial localization while also decreasing antiapoptotic Bcl-2 family members and their mitochondrial localization. (**c**) Simvastatin decreased mitochondrial membrane potential in treated myocardial atrial fibroblast. Cells were treated with simvastatin (10 μM, 72 h) and mitochondrial membrane potential were measured using JC-1 (***$P<0.001$) (see Materials and Methods section for details). (**d**–**f**) Mevalonate cascade inhibition decreased Bcl-2 expression via SAPK/JNK activation in myocardial atrial fibroblast. Cells were treated with simvastatin (10 μM) for indicated time points. Simvastatin increased SAPK/JNK phosphorylation (**d**) and (**e**) SAPK/JNK inhibitor (SB600123, 150 nM) significantly (**$P<0.01$) enhanced cell viability in the presence of simvastatin (10 μM, 72 h). Cells were pretreated with indicated concentration of SB600123 for 4 h and then co-treated with indicated concentration of simvastatin. Cell viability was measured using MTT assay. (**f**) SAPK/JNK inhibitor (SB600123, 150 nM) also inhibited the effect of simvastatin (10 μM, 72 h) on Bcl-2 expression

proteins (Bcl-2, Mcl-1 and Bcl-xL). The proapoptotic activity of PUMA is initiated by interaction with Bcl-2 in mitochondria,[38] and we have reported that PUMA localizes to mitochondria, reduces mitochondrial membrane potential, and induces intrinsic apoptosis pathways in human airway smooth muscle.[13] In our current study, decreased Bcl-2 in hATF was mediated, at least in part, by JNK/SAPK phosphorylation, and the JNK/SAPK inhibitor SP600125 was sufficient to prevent hATF death. These findings are consistent with work showing that Bcl-2, Bcl-xL and Bcl-w inhibit apoptosis, and that JNK/SAPK contributes to apoptosis through direct phosphorylation of Bcl-2 or transcriptional downregulation of Bcl-2 and c-IAP1.[39,40] Thus, it appears that statins modulate upstream regulatory events that can converge to alter Bcl-2 expression and distribution, and trigger intrinsic apoptosis in hAFTs.

Our findings reveal the existence of mevalonate cascade-linked regulatory axes that modulate ER proteases. Caspase-4 is a member of the group I family of caspases.[41] Its activation is associated with ER stress-induced cell death.[42,43] We show that simvastatin activates caspase-4 in hATF cells, and inhibition of caspase-4 suppresses caspase-3/-7 activation and intrinsic apoptosis-driven cell death.

In simvastatin-treated hATF cells we found marked cleavage and activation of cathepsin-B and -L, markers of lysosomal activation that can contribute to cell death.[44,45] Once released from lysosomes, cathepsins can cleave cellular substrates and act in concert with caspases to disrupt the mitochondrial transmembrane potential. A role for simvastatin-induced loss of lysosomal integrity and cathepsin-B and -L activation in apoptosis appears to exist, as we show they undergo cleavage, and cell death of hATF is

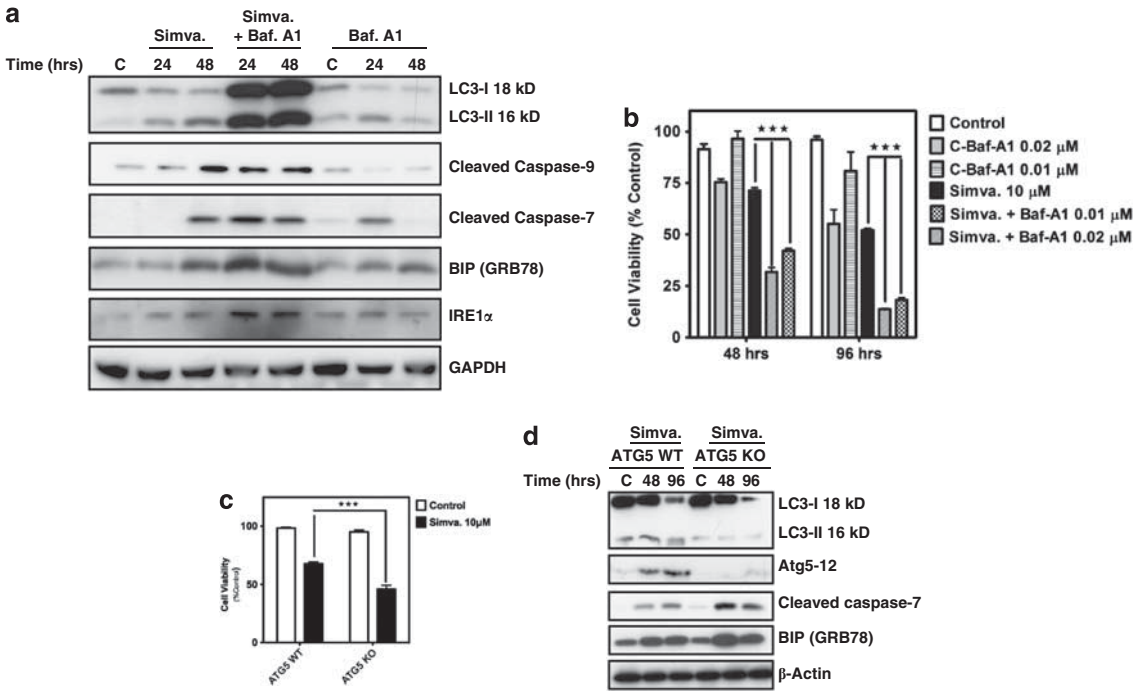

Figure 7 Mevalonate cascade-stimulated autophagy inhibition increases apoptosis and endoplasmic reticulum stress response and increases cell death (**a**) Myocardial atrial fibroblast were pretreated with bafilomycin-A1 (0.01 μM, 4 h) and then co-treated with simvastatin (10 μM) for indicated time point. Inhibition of autophagy flux increased LC3β II accumulation, caspase-3, -7 and -9 cleavage and IREα1 and BIP (GRP78) expression. (**b**) Bafilomycin-A1 (5 and 10 nM) pre and then cotreatment with simvastatin (10 μM) significantly increased simvastatin-induced loss of viability of myocardial atrial fibroblast (***$P<0.001$). Cell viability was measured using MTT assay. (**c** and **d**) Mouse embryo fibroblasts that express ATG5 and ATG5 knockout cells were treated with simvastatin (10 μM). ATG5 knockout cells exhibited significantly greater loss of cell viability (measured by MTT assay) in response to simvastatin (***$P<0.001$) (96 h) (**d**) and also increased caspase-7 cleavage and BIP expression. Equal loading was confirmed using β-actin

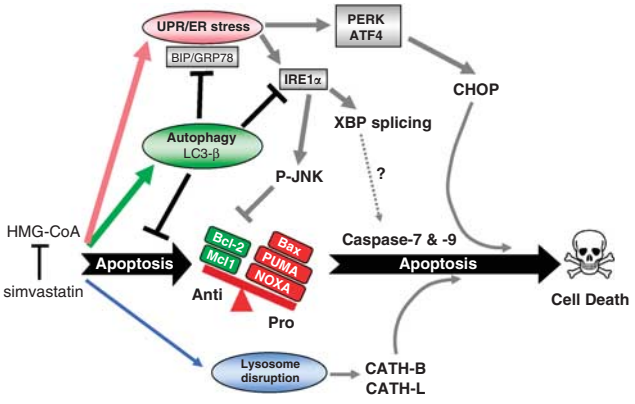

Figure 8 Schematic pathway highlighting major events in mevalonate cascade inhibition-induced cell death in hATF: HMG-CoA inhibition with simvastatin concomitantly induces apoptosis, autophagy and UPR/ER stress in hATF. Apoptosis initiation is driven by disruption of balance between pro and antiapoptotic Bcl-2 proteins. HMG-CoA inhibition also promotes UPR/ER stress as indicated by an increase in BIP/GRP78, and the activation of ATF4 and PERK, which in turn activate CHOP to support apoptosis. IREα1 is also activated, which leads to JNK phosphorylation (P-JNK) that contributes to loss of Bcl-2, further promoting apoptosis. IREα1 activation also triggers XBP1 splicing (but direct effects on apoptosis are not clear, as denoted by '?'). Inhibiting HMG-CoA also leads to leak of cathepsin (CATH)-B and CATH-L from lysosomes to augment apoptosis. HMG-CoA inhibition also induces autophagy flux (LC3-II accumulation), which has a suppressive role, negatively regulating apoptosis (cell viability, caspase-7 and -9) and UPR (BIP/GRP78, IREα1), albeit the autophagy response is not sufficient to ultimately prevent cell death

significantly suppressed by their respective selective inhibitors. In concert, simvastatin also induces autophagy, and Baf-A1 promotes accumulation of lipidated LC3; thus, our data indicate that autophagy flux is not directly affected by cathepsin release. This is consistent with findings in human HONE 1 nasopharyngeal carcinoma cells in which autophagy flux was unaffected by lysosome damage.[46] Our findings suggest the antiapoptotic and proapoptotic mechanisms of autophagy and lysosomal damage are mutually exclusive, though the hATF death response likely reflects the combined impact of each pathway (Figure 8).

During ATGs and organelles are engulfed by double-membrane vesicles to form autophagosomes that ultimately fuse with lysosomes, leading to content degradation by lysosomal enzymes.[47] Multiple studies show that apoptosis and autophagy are linked, and there is evidence for coordinated regulation of autophagy and ER stress in determining cell survival or death.[48–52] Indeed, autophagy is activated by a number of stressors including the UPR.[53,54] This is noteworthy because though our current work shows that statin exposure promotes multiple pathways that can lead to cell death, we also observed a marked induction of autophagy; a response that clearly tempers hATF demise. In human lung mesenchymal cells suppression of the mevalonate cascade underpins p53-regulated autophagy flux that attenuates intrinsic apoptosis.[12] The present study with hATF shows that chemical inhibition of autophagy flux has broader effects, as it attenuates statin-induced ER stress/

UPR (BIP/GRP78 and IREα1 expression) and activation of intrinsic apoptosis (capase-9, -7 and -3). Moreover, in MEF lacking ATG5, induction of markers of ER stress, UPR and apoptosis by mevalonate cascade inhibition were similarly blunted. Prevention of autophagosome degradation upon lysosome fusion with the vacuole H^+-ATPase inhibitor, Baf-A1 or preventing more proximal autophagosome formation in *ATG5* KO MEF was equally effective in enhancing simvastatin-induced cell death. In mammalian cells, autophagosomes form in the cytosol and then fuse with lysosomes under the control of distinct mechanisms.[55] Thus, simvastatin-induced autophagy in hATF involves enhanced autophagosome synthesis and flux and their regulation modulates cell stress responses that can lead to cell death.

Our study focuses on the impact of simultaneous initiation of autophagy, apoptosis and ER stress following inhibition of HMG-CoA reductase using statins, providing understanding of their interplay in homeostasis, survival and programmed death of primary hATFs. Although apoptosis is a tightly regulated cellular suicide program, autophagy can promote both cell survival and cell death. This study demonstrates that a clinically relevant inhibitor of the mevalonate cascade can induce hATF demise, a response that manifests from complex mechanisms involving co-regulation of ER stress, UPR and apoptosis. Coincident induction of autophagy determines the extent of the stress response and permissiveness for cell death, but in the cell system we employed this was not sufficient to prevent eventual cell death.

Materials and Methods

Reagents. Cell culture plasticware was obtained from Corning Inc. (Tewksbury, MA, USA). Cell culture media, propidium iodide, simvastatin, CA-074-ME, ZFF-FMK, mevalonate, cholesterol, MTT, rabbit anti-human/mouse/rat LC3β, and mouse anti-human/mouse BNIP3 were obtained from Sigma (Sigma-Aldrich, Oakville, CA, USA). Z-LEVD-FMK was purchased from Calbiochem :EMD Millipore (Darmstadt, Germany). Rabbit anti-human cleaved caspase-7,-3 JNK/SAPK, phospho JNK/SAPK, rabbit anti-Bak, Bax, PUMA, Bcl-2, Bid, Mcl-1, Bcl-XL Rac1/2/3, p21, RhoA, RhoC, GRP78 (BIP), IREα1, eif2α, phospho-eif2α, Atg5, Beclin-1 and Pan-cadherin were purchased from Cell Signaling Technology (Beverly, MA, USA). Rabbit anti-PERK, phospho-PERK, mouse anti-glyceraldehyde-3-phosphate dehydrogenase (GAPDH) and SP600125 were obtained from Santa Cruz Biotechnology Inc. (Santa Cruz, CA, USA). Rabbit anti-NOXA, anti-ATF6, anti-ATF4, anti-XBP1, anti-caspase-4, Cathepsin-B and mouse anti-Cathepsin L were obtained from Abcam (Cambridge, MA, USA). 5,5′,6,6′-tetrachloro-1,1′,3,3′-tetraethylbenzimidazolylcarbocyanine iodide (JC-1), and Lysotracker Red, were obtained from Invitrogen Molecular Probes (Burlington, ON, Canada). Casapase-Glo-3/7 assay was purchased from Promega (Madison, WI, USA).

Primary human atrial fibroblast (hATF) cell culture preparation. Approval was obtained from the Bannatyne Campus Research Ethics Board of the University of Manitoba for the collection of atrial tissue from patients undergoing a cardiac surgical procedure. Written informed consent was obtained from each patient before tissue collection. Fragments of atrial tissue were subjected to collagenase digestion to isolate cardiac myofibroblasts. Minced atrial tissue was treated with 2 mg/ml collagenase II (Worthington Biochemical Corp., Lakewood, NJ, USA) in SMEM media (GIBCO/Life Technologies, Burlington, ON, Canada) and incubated for 3 h at 37 °C. Collagenase was neutralized by the addition of an equal volume of medium containing 20% fetal bovine serum (FBS) and liberated cells were collected by centrifugation at 2000 r.p.m. for 7 min. Cells were resuspended in fresh complete medium containing 20% FBS, seeded onto plastic culture dishes and incubated at 37 °C in 5% CO_2 and 95% humidity. The digestion was repeated with the remaining tissue pieces. Non-adherent cells (myocytes) were removed the next day and fresh medium was added to the adherent cells and replaced every 3 or 4 days.

MTT assay. Cytotoxicity of simvastatin towards the hATF cells was determined by MTT assays as previously described.[12] In experiments investigating the effects of mevalonate (0–2.5 mM), cholesterol (0–50 μM), CA-074-ME and ZFF-FMK (0–50 μM), Z-LEVD-FMK (0–25 μM) and SP600125 (10 μM), hATF cells were pretreated with the indicated concentration of the inhibitors or chemical (4 h) and then co-treated with indicated concentrations of simvastatin for experimental time points. For each experiment time-matched vehicle controls were performed.

Luminescence caspase activity assays. Luminometric assays Caspase-Glo-3/7 (Promega, Nepean, ON, Canada) was used to measure the proteolytic activity of caspase-3/7 (DEVD-ase). The assays were performed according to manufactures instructions with some modification as detailed in our previous work.[13]

Quantitative analysis of nuclear fluorescence using laser scanning cytometry. Human atrial fibroblast cells were grown to 80% confluence in Dulbeco's Modified Eagle Medium (DMEM) supplemented with 10% FBS on glass coverslips. At confluence, the medium was replaced with DMEM containing reduced serum (0.5% FBS) for 48 h after which cells were incubated in serum reduced medium with or without simvastatin (10 μM). Fluorescent labeling of live cell nuclei was carried out by incubation in Hank's balanced salt solution containing 5 μg/ml Hoechst 33 342 dye (15 min, 37 °C). Quantitation and analysis of nuclear DNA fluorescence was carried out using a laser scanning cytometer (Compucyte Corp., Westwood, MA, USA) as described before.[13]

Analysis of cellular morphology. We assessed cell viability based on gross cellular appearance (chromatin condensation and cell shrinkage) and the effect of mevalonate on simvastatin (10 μM) cytotoxicity at indicated time points on hATF cells grown on 12-well plates by phase contrast microscopy (Olympus CK40; Olympus Canada, Mississauga, ON, Canada) using a DP10 CCD digital camera to capture images.

Membrane anchoring of Rho GTPases. For determination of membrane anchoring of prenylated Rho and Rac GTPases, hATF cells were cultured in DMEM/0.5% FBS in the presence or absence of simvastatin (10 μM). After washing cells were scraped in ice-cold buffer (10 mM Tris-HCl, pH 7.5, 0.1 mM EDTA, 0.1 mM EGTA, 1 mM dithiothreitol and protease inhibitor cocktail), sonicated on ice 3 $\times$ for 5 s, and then the homogenate was separated into cytoplasmic and membrane fractions by ultracentrifugation (100 000 $\times$ *g* for 35 min). The membrane fractions were solublized in dissociation buffer (50 mM Tris-HCl, pH 7.5, 0.15 M NaCl, 1 mM dithiothreitol, 1% SDS, 1 mM EDTA, 1 mM EGTA, protease inhibitor cocktail) and subsequently size fractioned by SDS-PAGE for immunoblot analysis using anti-Rac1/2/3 and anti-RhoA, and RhoC primary antibodies (Cell Signaling Technology).

Mitochondrial membrane potential assay. This assay was performed using a mitochondria-specific cationic dye (JC-1), which undergoes potential-dependent accumulation in mitochondria. hATF cells were seeded in black clear-bottom 96-well plates. Following treatment with 10 μM simvastatin for different time intervals as indicated, mitochondrial membrane potential was measured as previously described.[13]

Immunoblotting. Blotting was used to detect cleaved caspase-3, -9, -7, Bcl-2, Bid, PUMA, NOXA, Bax, ATF6, caspase-4, ATF4, IREα1, eif2α, phospho-eif2α, PERK, phospho-PERK, Atg5-12, LC3β, beclin-1, Cathepsin-B, Cathepsin L, Mn-SOD2, Pan-Cadherin and GAPDH. Briefly, cells were washed and protein extracts were prepared in lysis buffer (20 mM Tris-HCl (pH 7.5), 0.5% Nonidet P-40, 0.5 mM PMSF, 100 μM β-glycerol 3-phosphate and 0.5% protease inhibitor cocktail). After centrifugation (13 000 $\times$ *g*, 10 min), supernatant protein content was determined by Lowry protein assay, then proteins were size fractionated by SDS-PAGE and transferred onto nylon membranes under reducing conditions. After blocking membranes with non-fat-dried milk and Tween 20, blots were incubated overnight with the primary antibodies at 4 °C. HRP-conjugated secondary antibody incubation was for 1 h at RT, then blots were developed with enhanced chemiluminescence regents (Amersham-Pharmacia Biotech/GE Healthcare Life Sciences, Baie d'Urfe PQ, Canada).

Immunocytochemistry, confocal imaging and electron microscopy. For immunocytochemistry, hATF cells were grown overnight on coverslips and then treated with simvastatin (10 μM) or vehicle for 72 h.

Lysosomes were stained with Lysotracker red (Molecular Probes/Life Technologies, Burlington, ON, Canada) (100 nM, 10 min) before fixation (4% paraformaldehyde/120 mM sucrose) and permeabilization (3% Triton X-100). Cells were then incubated with rabbit anti-LC3β IgG (1 : 200) with corresponding fluorochrome-conjugated secondary antibodies. The fluorescent images were then observed and analyzed using an Olympus FluoView multi-laser confocal microscope. For transmission electron microscopy (TEM), cells were fixed (2.5% glutaraldehyde in PBS (pH 7.4) for 1 h at 4 °C) and post-fixed (1% osmium tetroxide) before embedding in Epon. TEM was performed with a Philips CM10, at 80 kV, on ultra-thin sections (100 nm on 200-mesh grids) stained with uranyl acetate and counterstained with lead citrate.

Subcellular fractionation. Following induction of cell death using simvastatin (10 μM), cytosolic, mitochondrial and nuclear fractions were generated using a digitonin-based subcellular fractionation technique, essentially as described previously.[13] Briefly, 10^7 cells were harvested by centrifugation at $800 \times g$, washed in PBS pH 7.2 and re-pelleted. Cells were digitonin-permeabilized for 5 min on ice at a density of 3×10^7/ml in cytosolic extraction buffer (250 mM sucrose, 70 mM KCl, 137 mM NaCl, 4.3 mM Na_2HPO4, 1.4 mM KH_2PO_4 pH 7.2, 100 μM PMSF, 10 μg/ml leupeptin, 2 μg/ml aprotinin, containing 200 μg/ml digitonin). Plasma membrane permeabilization of cells was confirmed by staining in a 0.2% trypan blue solution. Cells were then centrifuged at $1000 \times g$ for 5 min at 4 °C. The supernatants (cytosolic and mitochondrial fractions) were saved and the pellets solubilized in the same volume of nuclear lysis buffer, followed by pelletting at $12\,500 \times g$ for 10 min at 4 °C. The mitochondria were separated from the cytosolic fraction by pelleting at $13\,000 \times g$. The pellets were solubilized in equal amount of mitochondrial lysis buffer (50 mM Tris pH 7.4, 150 mM NaCl, 2 mM EDTA, 2 mM EGTA, 0.2 % Triton X-100, 0.3% NP-40, 100 μM PMSF, 10 μg/ml leupeptin, 2 μg/ml aprotinin). For the detection of proteins, equal amounts of fractionated protein were supplemented with 5 $\times$ SDS-PAGE loading buffer, subjected to standard 12% SDS-PAGE and transferred to nitrocellulose membranes.

Statistical analysis. The results were expressed as means $\pm$ S.D. and statistical differences were evaluated by one-way or two-way ANOVA followed by Tukey's or Bonferroni's *post hoc* test, using Graph Pad Prism 5.0 (Graph Pad Software Inc., La Jolla, CA, USA). $P<0.05$ was considered significant. In all experiments data were collected in triplicate from at least three cell lines unless otherwise indicated.

Conflict of Interest

The authors declare no conflict of interest.

Acknowledgements. This work was supported by grants from the Canadian Institutes of Health Research (CIHR) (AJH and IMCD), GlaxoSmithKline Collaborative Innovation Research Fund, Manitoba Institute of Child Health (AJH), Canada Foundation for Innovation (AJH and DHF), and the St Boniface Hospital Foundation (DHF). SG is supported by Parker B Francis Fellowship in Pulmonary Research. PS is supported by a CIHR studentship. TK acknowledges the support by the Natural Sciences and Engineering Research Council of Canada (NSERC). BY is supported by a MHRC postdoctoral fellowship. AJH holds a Canada Research Chair in Airway Cell and Molecular Biology. We acknowledge Professor Marek J Los for providing MEF Atg5 KO cells.

1. Cohn JN, Ferrari R, Sharpe N. Cardiac remodeling–concepts and clinical implications: a consensus paper from an international forum on cardiac remodeling. Behalf of an international forum on cardiac remodeling. *J Am Coll Cardiol* 2000; **35**: 569–582.
2. Eghbali M. Cardiac fibroblasts: function, regulation of gene expression, and phenotypic modulation. *Basic Res Cardiol* 1992; **87**(Suppl 2): 183–189.
3. Cunnington RH, Wang B, Ghavami S, Bathe KL, Rattan SG, Dixon IM. Antifibrotic properties of c-Ski and its regulation of cardiac myofibroblast phenotype and contractility. *Am J Physiol Cell Physiol* 2011; **300**: C176–C186.
4. Werner N, Nickenig G, Laufs U. Pleiotropic effects of HMG-CoA reductase inhibitors. *Basic Res Cardiol* 2002; **97**: 105–116.
5. Porter KE, Turner NA. Statins and myocardial remodelling: cell and molecular pathways. *Expert Rev Mol Med* 2011; **13**: e22.
6. Correale M, Brunetti ND, Totaro A, Montrone D, Russo AR, Fanigliulo AM *et al.* Statin therapy blunts inflammatory activation and improves prognosis and left ventricular performance assessed by tissue doppler imaging in subjects with chronic ischemic heart failure: results from the Daunia Heart Failure Registry. *Clinics (Sao Paulo)* 2011; **66**: 777–784.
7. Zhang L, Zhang S, Jiang H, Sun A, Zou Y, Ge J. Effects of statin treatment on cardiac function in patients with chronic heart failure: a meta-analysis of randomized controlled trials. *Clin Cardiol* 2011; **34**: 117–123.
8. Dai Y, Khanna P, Chen S, Pei XY, Dent P, Grant S. Statins synergistically potentiate 7-hydroxystaurosporine (UCN-01) lethality in human leukemia and myeloma cells by disrupting Ras farnesylation and activation. *Blood* 2007; **109**: 4415–4423.
9. Hamada M, Miki T, Iwai S, Shimizu H, Yura Y. Involvement of RhoA and RalB in geranylgeranyltransferase I inhibitor-mediated inhibition of proliferation and migration of human oral squamous cell carcinoma cells. *Cancer Chemother Pharmacol* 2011; **68**: 559–569.
10. Kamigaki M, Sasaki T, Serikawa M, Inoue M, Kobayashi K, Itsuki H *et al.* Statins induce apoptosis and inhibit proliferation in cholangiocarcinoma cells. *Int J Oncol* 2011; **39**: 561–568.
11. Chen JC, Wu ML, Huang KC, Lin WW. HMG-CoA reductase inhibitors activate the unfolded protein response and induce cytoprotective GRP78 expression. *Cardiovasc Res* 2008; **80**: 138–150.
12. Ghavami S, Mutawe MM, Sharma P, Yeganeh B, McNeill KD, Klonisch T *et al.* Mevalonate cascade regulation of airway mesenchymal cell autophagy and apoptosis: a dual role for p53. *PloS one* 2011; **6**: e16523.
13. Ghavami S, Mutawe MM, Hauff K, Stelmack GL, Schaafsma D, Sharma P *et al.* Statin-triggered cell death in primary human lung mesenchymal cells involves p53-PUMA and release of Smac and Omi but not cytochrome *c. Biochim Biophys Acta* 2010; **1803**: 452–467.
14. Ghavami S, Mutawe MM, Schaafsma D, Yeganeh B, Unruh H, Klonisch T *et al.* Geranylgeranyl transferase 1 modulates autophagy and apoptosis in human airway smooth muscle. *Am J Physiol Lung Cell Mol Physiol* 2012; **302**: L420–L428.
15. Ali BR, Nouvel I, Leung KF, Hume AN, Seabra MC. A novel statin-mediated "prenylation block-and-release" assay provides insight into the membrane targeting mechanisms of small GTPases. *Biochem Biophys Res Commun* 2010; **397**: 34–41.
16. Araki M, Motojima K. Hydrophobic statins induce autophagy in cultured human rhabdomyosarcoma cells. *Biochem Biophys Res Commun* 2008; **367**: 462–467.
17. Toepfer N, Childress C, Parikh A, Rukstalis D, Yang W. Atorvastatin induces autophagy in prostate cancer PC3 cells through activation of LC3 transcription. *Cancer Biol Ther* 2011; **12**: 691–699.
18. Hanada T, Noda NN, Satomi Y, Ichimura Y, Fujioka Y, Takao T *et al.* The Atg12-Atg5 conjugate has a novel E3-like activity for protein lipidation in autophagy. *J Biol Chem* 2007; **282**: 37298–37302.
19. Ugland H, Naderi S, Brech A, Collas P, Blomhoff HK. cAMP induces autophagy via a novel pathway involving ERK, cyclin E and Beclin 1. *Autophagy* 2011; **7**: 1199–1211.
20. Szegezdi E, Logue SE, Gorman AM, Samali A. Mediators of endoplasmic reticulum stress-induced apoptosis. *EMBO Reports* 2006; **7**: 880–885.
21. Tsai B, Ye Y, Rapoport TA. Retro-translocation of proteins from the endoplasmic reticulum into the cytosol. *Nat Rev Mol Cell Biol* 2002; **3**: 246–255.
22. Yang Z, Zhang XQ, Dinney CN, Benedict WF. Direct cytotoxicity produced by adenoviral-mediated interferon alpha gene transfer in interferon-resistant cancer cells involves ER stress and caspase 4 activation. *Cancer Gene Ther* 2011; **18**: 609–616.
23. Yamamuro A, Kishino T, Ohshima Y, Yoshioka Y, Kimura T, Kasai A *et al.* Caspase-4 directly activates caspase-9 in endoplasmic reticulum stress-induced apoptosis in SH-SY5Y cells. *J Pharmacol Sci* 2011; **115**: 239–243.
24. Salminen A, Kauppinen A, Suuronen T, Kaarniranta K, Ojala JER. stress in Alzheimer's disease: a novel neuronal trigger for inflammation and Alzheimer's pathology. *J Neuroinflamm* 2009; **6**: 41.
25. Binet F, Chiasson S, Girard D. Evidence that endoplasmic reticulum (ER) stress and caspase-4 activation occur in human neutrophils. *Biochem Biophys Res Commun* 2010; **391**: 18–23.
26. Daniel PT, Schulze-Osthoff K, Belka C, Guner D. Guardians of cell death: the Bcl-2 family proteins. *Essays Biochem* 2003; **39**: 73–88.
27. Mishra S, Mishra JP, Kumar A. Activation of JNK-dependent pathway is required for HIV viral protein R-induced apoptosis in human monocytic cells: involvement of antiapoptotic BCL2 and c-IAP1 genes. *J Biol Chem* 2007; **282**: 4288–4300.
28. Phillips AR, Suttangkakul A, Vierstra RD. The ATG12-conjugating enzyme ATG10 Is essential for autophagic vesicle formation in *Arabidopsis thaliana. Genetics* 2008; **178**: 1339–1353.
29. Blanco-Colio LM, Villa A, Ortego M, Hernandez-Presa MA, Pascual A, Plaza JJ *et al.* 3-Hydroxy-3-methyl-glutaryl coenzyme A reductase inhibitors, atorvastatin and simvastatin, induce apoptosis of vascular smooth muscle cells by downregulation of Bcl-2 expression and Rho A prenylation. *Atherosclerosis* 2002; **161**: 17–26.
30. Zhao H, Liao Y, Minamino T, Asano Y, Asakura M, Kim J *et al.* Inhibition of cardiac remodeling by pravastatin is associated with amelioration of endoplasmic reticulum stress. *Hypertens Res* 2008; **31**: 1977–1987.
31. Xu GQ, Huang WF, Liu H, Yang YC, Liu W. [Simvastatin-induced apoptosis of K562 cells is mediated by endoplasmic reticulum stress]. *Yao Xue Xue Bao* 2008; **43**: 371–377.
32. Schweitzer M, Mitmaker B, Obrand D, Sheiner N, Abraham C, Dostanic S *et al.* Atorvastatin mediates increases in intralesional BAX and BAK expression in human end-stage abdominal aortic aneurysms. *Can J Physiol Pharmacol* 2009; **87**: 915–922.

33. Hetz C, Martinon F, Rodriguez D, Glimcher LH. The unfolded protein response: integrating stress signals through the stress sensor IRE1alpha. *Physiol Rev* 2011; **91**: 1219–1243.
34. Wang Q, Mora-Jensen H, Weniger MA, Perez-Galan P, Wolford C, Hai T *et al.* ERAD inhibitors integrate ER stress with an epigenetic mechanism to activate BH3-only protein NOXA in cancer cells. *Proc Natl Acad Sci USA* 2009; **106**: 2200–2205.
35. Fornace AJ Jr., Alamo I Jr., Hollander MC. DNA damage-inducible transcripts in mammalian cells. *Proc Natl Acad Sci USA* 1988; **85**: 8800–8804.
36. Ma Y, Brewer JW, Diehl JA, Hendershot LM. Two distinct stress signaling pathways converge upon the CHOP promoter during the mammalian unfolded protein response. *J Mol Biol* 2002; **318**: 1351–1365.
37. Puthalakath H, O'Reilly LA, Gunn P, Lee L, Kelly PN, Huntington ND *et al.* ER stress triggers apoptosis by activating BH3-only protein Bim. *Cell* 2007; **129**: 1337–1349.
38. Yee KS, Vousden KH. Contribution of membrane localization to the apoptotic activity of PUMA. *Apoptosis* 2008; **13**: 87–95.
39. Maundrell K, Antonsson B, Magnenat E, Camps M, Muda M, Chabert C *et al.* Bcl-2 undergoes phosphorylation by c-Jun N-terminal kinase/stress-activated protein kinases in the presence of the constitutively active GTP-binding protein Rac1. *J Biol Chem* 1997; **272**: 25238–25242.
40. Davis RJ. Signal transduction by the JNK group of MAP kinases. *Cell* 2000; **103**: 239–252.
41. Van de Craen M, Vandenabeele P, Declercq W, Van den Brande I, Van Loo G, Molemans F *et al.* Characterization of seven murine caspase family members. *FEBS Lett* 1997; **403**: 61–69.
42. Badiola N, Penas C, Minano-Molina A, Barneda-Zahonero B, Fado R, Sanchez-Opazo G *et al.* Induction of ER stress in response to oxygen-glucose deprivation of cortical cultures involves the activation of the PERK and IRE-1 pathways and of caspase-12. *Cell Death Dis* 2011; **2**: e149.
43. Yamamuro A, Kishino T, Ohshima Y, Yoshioka Y, Kimura T, Kasai A *et al.* Caspase-4 directly activates caspase-9 in endoplasmic reticulum stress-induced apoptosis in SH-SY5Y cells. *J Pharmacol Sci* 2011; **115**: 239–243.
44. Boya P, Gonzalez-Polo RA, Poncet D, Andreau K, Vieira HL, Roumier T *et al.* Mitochondrial membrane permeabilization is a critical step of lysosome-initiated apoptosis induced by hydroxychloroquine. *Oncogene* 2003; **22**(): 3927–3936.
45. Boya P, Cohen I, Zamzami N, Vieira HL, Kroemer G. Endoplasmic reticulum stress-induced cell death requires mitochondrial membrane permeabilization. *Cell Death Differ* 2002; **9**: 465–467.
46. Chen KL, Chang WS, Cheung CH, Lin CC, Huang CC, Yang YN *et al.* Targeting cathepsin S induces tumor cell autophagy via the EGFR-ERK signaling pathway. *Cancer Lett* 2012; **317**: 89–98.
47. Mizushima N, Levine B, Cuervo AM, Klionsky DJ. Autophagy fights disease through cellular self-digestion. *Nature* 2008; **451**: 1069–1075.
48. Filippi-Chiela EC, Villodre ES, Zamin LL, Lenz G. Autophagy interplay with apoptosis and cell cycle regulation in the growth inhibiting effect of resveratrol in glioma cells. *PLoS One* 2011; **6**: e20849.
49. Shi YH, Ding ZB, Zhou J, Hui B, Shi GM, Ke AW *et al.* Targeting autophagy enhances sorafenib lethality for hepatocellular carcinoma via ER stress-related apoptosis. *Autophagy* 2011; **7**: 1159–1172.
50. Scheper W, Nijholt DA, Hoozemans JJ. The unfolded protein response and proteostasis in Alzheimer disease: preferential activation of autophagy by endoplasmic reticulum stress. *Autophagy* 2011; **7**: 910–911.
51. Kario E, Amar N, Elazar Z, Navon A. A new autophagy-related checkpoint in the degradation of an ERAD-M target. *J Biol Chem* 2011; **286**: 11479–11491.
52. Petrovski G, Das S, Juhasz B, Kertesz A, Tosaki A, Das DK. Cardioprotection by endoplasmic reticulum stress-induced autophagy. *Antioxid Redox Signal* 2011; **14**: 2191–2200.
53. Ogata M, Hino S, Saito A, Morikawa K, Kondo S, Kanemoto S *et al.* Autophagy is activated for cell survival after endoplasmic reticulum stress. *Mol Cell Biol* 2006; **26**: 9220–9231.
54. Yorimitsu T, Nair U, Yang Z, Klionsky DJ. Endoplasmic reticulum stress triggers autophagy. *J Biol Chem* 2006; **281**: 30299–30304.
55. Rubinsztein DC, Cuervo AM, Ravikumar B, Sarkar S, Korolchuk V, Kaushik S *et al.* In search of an "autophagomometer". *Autophagy* 2009; **5**: 585–589.